The $A(K^-_{stop}, \Lambda d)A'$ reaction, a tool to observe $[\overline{K}NNN]$ clusters

The FINUDA Collaboration

M. Agnello[1,9], G. Beer[2], L. Benussi[3], M. Bertani[3], H.C. Bhang[4], S. Bianco[3], G. Bonomi[5,13], E. Botta[6,9], M. Bregant[7,15], T. Bressani[6,9], S. Bufalino[6,9], L. Busso[8,9], D. Calvo[9], P. Camerini[7,15], M. Caponero[10], P. Cerello[9], B. Dalena[11,12], F. De Mori[6,9], G. D'Erasmo[11,12], D. Di Santo[11,12], D. Elia[12], F.L. Fabbri[3], D. Faso[8,9], A. Feliciello[9], A. Filippi[9], V. Filippini[13†], R.A. Fini[12], E.M. Fiore[11,12], H. Fujioka[14], P. Gianotti[3], N. Grion[15], O. Hartmann[3], A. Krasnoperov[16], V. Lenti[12], V. Lucherini[3], V. Manzari[12], S. Marcello[6,9], T. Maruta[14], N. Mirfakhrai[17], O. Morra[18,9], T. Nagae[19], H. Outa[20], E. Pace[3], M. Pallotta[3], M. Palomba[11,12], A. Pantaleo[12], A. Panzarasa[13], V. Paticchio[12], S. Piano[15,a], F. Pompili[3], R. Rui[7,15], G. Simonetti[11,12], H. So[4], V. Tereshchenko[16], S. Tomassini[3], A. Toyoda[19], R. Wheadon[9], and A. Zenoni[5,13]

[1] Dipartimento di Fisica, Politecnico di Torino, Corso Duca degli Abruzzi 24, Torino, Italy
[2] University of Victoria, Finnerty Rd., Victoria, Canada
[3] Laboratori Nazionali di Frascati dell'INFN, via E. Fermi 40, Frascati, Italy
[4] Department of Physics, Seoul National University, 151-742 Seoul, Korea
[5] Dipartimento di Meccanica, Università di Brescia, via Valotti 9, Brescia, Italy
[6] Dipartimento di Fisica Sperimentale, Università di Torino, Italy
[7] Dipartimento di Fisica, Università di Trieste, Italy
[8] Dipartimento di Fisica Generale, Università di Torino, Italy
[9] INFN Sezione di Torino, via P. Giuria 1, Torino, Italy
[10] ENEA C.R. Frascati, via E. Fermi 45, Frascati, Italy
[11] Dipartimento InterAteneo di Fisica, Università di Bari, Italy
[12] INFN Sezione di Bari, via Amendola 173, Bari, Italy
[13] INFN Sezione di Pavia, via Bassi 6, Pavia, Italy
[14] Department of Physics, University of Tokyo, Bunkyo Tokyo 113-0033, Japan
[15] INFN Sezione di Trieste, via Valerio 2, Trieste, Italy
[16] JINR Dubna, Moscow region, Russia
[17] Department of Physics, Shahid Behesty University, 19834 Teheran, Iran
[18] INAF-IFSI Sezione di Torino, Corso Fiume 4, Torino, Italy
[19] High Energy Accelerator Research Organization (KEK), Tsukuba, Ibaraki 305-0801, Japan
[20] RIKEN, Wako, Saitama 351-0198, Japan

Paper reprinted from Eur. Phys. J. A with permission

Abstract. This work presents experimental results obtained from a study of the $K^-_{stop}A \to \Lambda dA'$ reaction, where $A = {}^6$Li. The study concerns the distributions of the Λd invariant mass, which allows us to determine the structure of bound $[K^-ppn]$ systems in nuclei. A candidate of such clusters is identified in the present measurement, and its mass (binding energy), decay width and yield are reported. The experiment was performed at the DAΦNE ϕ-facility (LNF) by using the FINUDA spectrometer. The study depended on the capability of FINUDA to reconstruct the traces of all the particles involved in the decay of the nuclear cluster.

PACS. 21.45.+v Few-body systems – 21.80.+a Hypernuclei – 25.80.Nv Kaon-induced reactions

1 Introduction

This paper investigates the invariant-mass spectra of Λd pairs, produced in the kaon absorption reaction $K^-_{stop}A \to \Lambda(1116)d\,A'$, where $A = {}^6$Li and A' is the residual nucleus, a system of 3 nucleons not necessarily bound. The present study follows an earlier Λp survey on light and medium-light nuclei [1], which hinted that negative kaons gather nucleons of the nucleus to form bound systems; *i.e.*, $K^-_{stop}pp \to [K^-pp] \to \Lambda p$. The present discussion is

[a] e-mail: stefano.piano@ts.infn.it
[†] Deceased.

about the dynamics of $[\overline{K}NNN]$ clusters in ^{6}Li, which is pursued by studying the Λd decay channel.

2 The data analysis

In the FINUDA experiment negative kaons are produced by the DAΦNE collider at LNF via initial e^+e^- collisions, which produce $\Phi(1020)$ mesons which are nearly at rest. The prompt decay of Φ's in the $\Phi \to K^+K^-$ channel (B.R. $\sim 50\%$) is the source of the ~ 16 MeV kaons, which are emitted back to back. When a negative kaon initiates the reaction process, the associated positive kaon ensures the identification of the K^-K^+ event. Negative kaons are slowed down to rest in solid targets; the targets chosen for the first FINUDA data taking were: $2\times^6$Li, $1\times^7$Li, $3\times^{12}$C, $1\times^{27}$Al and $1\times^{51}$V. The low energy of the kaons favors the use of thin targets, *i.e.*, as thin as $0.213\,\mathrm{g/cm^2}$ for ^{6}Li.

The momentum of the particles involved in the K^- absorption and decay processes, namely π's, p's and d's, is measured by the tracking system of FINUDA [2], which consists of two cylindrical layers of silicon microstrip detectors, with the outside layer 7.5 cm from the e^+e^- crossing beams, two layers of low-mass wire chambers, and a final stack of straw tubes whose inner layer is set at 111.0 cm from the crossing beams.

The charged particles produced in the absorption (or decay) process are mass identified by their specific energy deposited ($\mathrm{d}E/\mathrm{d}x$) into some active layers of the spectrometer. In fact, a coherent response of a minimum of 3 $\mathrm{d}E/\mathrm{d}x$ layers is required to identify a particle as a pion, a proton or a deuteron. In order to check the contamination of PID's, the mass of the particles is independently determined by measuring their time of flight. The contamination in the charged-particle identifications turns out to be less than 4%. This capability of FINUDA combined with the tracking permits the full reconstruction of the $K^-_{stop}\,A \to \Lambda d\,A'$ reaction to be performed, with the only exception of A'.

An initial K^-d vertex determines the stopping position of the negative kaon in the target (A). In turn, a Λ hyperon is reconstructed via the $\Lambda \to \pi^-p$ decay. These particles form a secondary vertex, which is separated from the K^-_{stop} vertex. A minimum distance (1 mm) is therefore required between the two vertices. The Λd correlation is ensured since both particles belong to the same reconstructed event.

Figure 1 depicts the $p\pi^-$ pairs invariant-mass distribution when they are detected in coincidence with a deuteron. $\Lambda(1116)$ appears as a peak standing out over a low background. Such a clean discrimination of Λ's is the result a good energy resolution ($\Gamma_\Lambda/m_\Lambda = 0.8\%$) combined with the topology of the π^-pd events. In this case, the topology requires that the $\Lambda \to \pi^-p$ decays are correlated with the K^-d vertices. It is worthwhile noting that the Λ invariant mass of the $K^-_{stop}A \to \Lambda dA'$ reaction appears to be almost free from the background generated by the uncorrelated π^-p pairs.

Λ hyperons are detected from $\sim 140\,\mathrm{MeV}/c$ (threshold) up to $800\,\mathrm{MeV}/c$. Deuterons from the Λd channel are analyzed starting from $\sim 300\,\mathrm{MeV}/c$ (threshold) up to momenta of about $800\,\mathrm{MeV}/c$. Both Λ's and d's are measured with a resolution better than $\Delta p/p < 2\%$. The wide angular acceptance of FINUDA allows for $0^\circ \le \Theta_{\Lambda d} < 180^\circ$ Λd opening angle measurements. Finally, the spectra presented are corrected for the spectrometer acceptance, which is a source of systematic uncertainty.

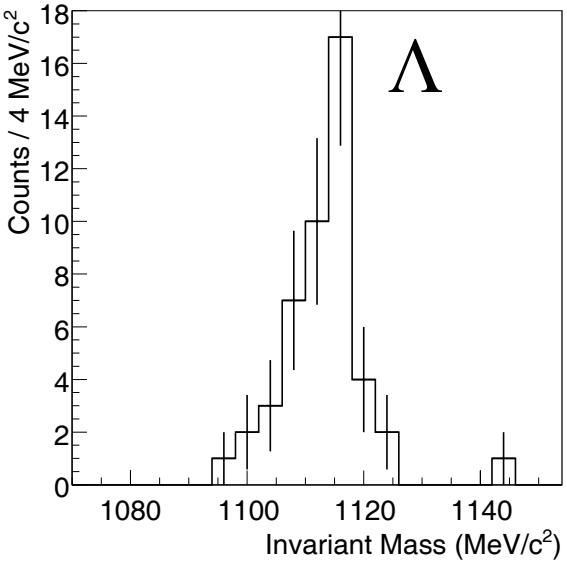

Fig. 1. Invariant-mass distribution of $p\pi^-$ pairs from the $^6\mathrm{Li}(K^-_{stop}, p\pi^-d)A'$ reaction, where a coincidence with a deuteron is required.

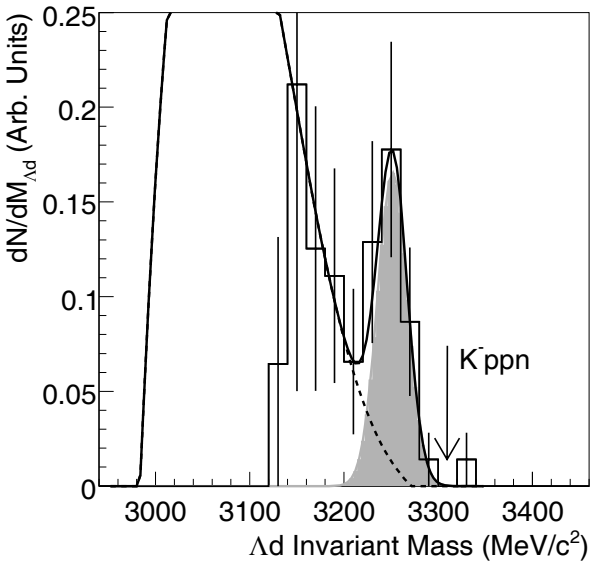

Fig. 2. Invariant-mass distribution of Λd pairs from the $^6\mathrm{Li}(K^-_{stop}, \Lambda d)A'$ reaction (open histogram). The solid curve is the global fit, which is composed by the background distribution (dashed curve) and the normal fitting to the bump (grey-filled curve). The arrow indicates the overall mass of the unbound K^-ppn system.

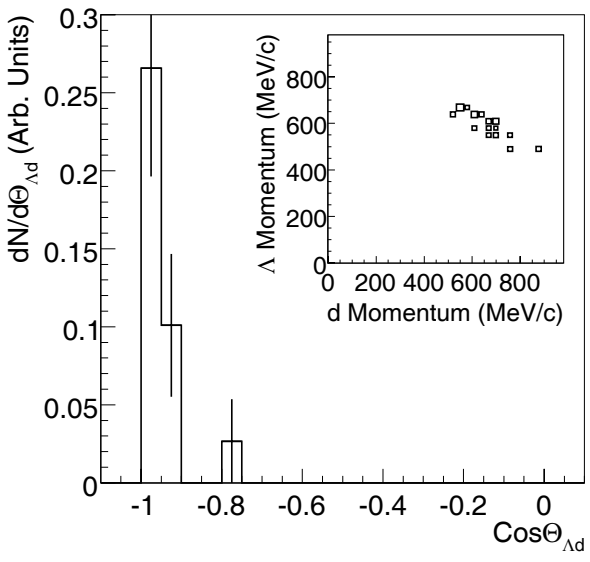

Fig. 3. Opening-angle distribution of Λd pairs from ^{6}Li for the $3220 \leq m_{\Lambda d} \leq 3280\,\mathrm{MeV}/c^2$ events. Inset, correlation between Λ and d momentum for the $3220 \leq m_{\Lambda d} \leq 3280\,\mathrm{MeV}/c^2$ events on ^{6}Li.

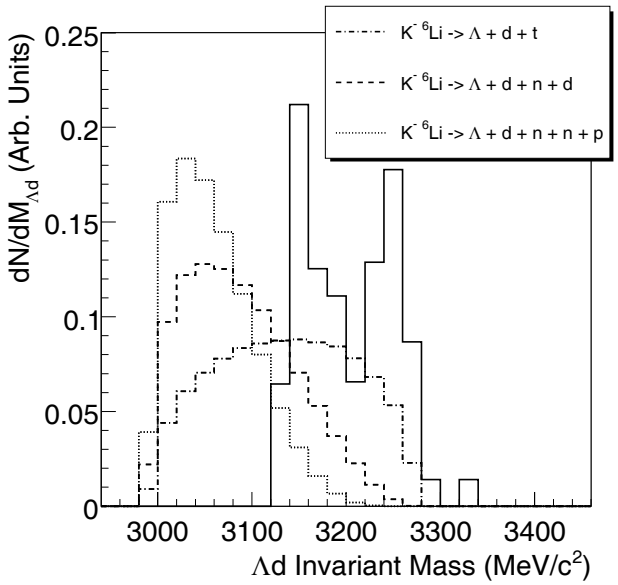

Fig. 4. Invariant-mass distribution of Λd pairs from the phase space simulation of $^6\mathrm{Li}(K^-_{stop}, \Lambda d)t$ (dot-dashed histogram), $^6\mathrm{Li}(K^-_{stop}, \Lambda d)nd$ (dashed histogram) and $^6\mathrm{Li}(K^-_{stop}, \Lambda d)nnp$ (dotted histogram) reactions. The solid histogram is the same of fig. 2.

Figure 2 shows the Λd invariant mass ($m_{\Lambda d}$) for ^{6}Li, its strength is below the overall mass of the unbound K^-ppn system, indicated by an arrow in fig. 2. A broad bump at $m_{\Lambda d} \sim 3250\,\mathrm{MeV}/c^2$ emerges, whose nature is investigated. The lack of data below $3120\,\mathrm{MeV}/c^2$ is due to the poor statistics and the low acceptance of the apparatus, which drops by more than a factor three between $3250\,\mathrm{MeV}/c^2$ and $3130\,\mathrm{MeV}/c^2$. Therefore, with the present data it is not possible to discuss the region around $3140\,\mathrm{MeV}/c^2$, where the FOPI Collaboration observed a resonance by means of heavy-ion collisions [3].

In order to obtain the position of the bump at $3250\,\mathrm{MeV}/c^2$ ($m_{\Lambda d}$), the width and the yield ($Y_{\Lambda d}$), the invariant-mass spectrum is fitted with a global function given by the sum of the background and the normal distribution. The background distribution is composed by the three polynomial parametrizations of the phase space simulations of $^6\mathrm{Li}(K^-_{stop}, \Lambda d)t$, $^6\mathrm{Li}(K^-_{stop}, \Lambda d)nd$, $^6\mathrm{Li}(K^-_{stop}, \Lambda d)nnp$ reactions, shown in fig. 4 and discussed in sect. 3. The fit results are $m_{\Lambda d} = (3251 \pm 6)\,\mathrm{MeV}/c^2$, $\Gamma_{\Lambda d} = (36.6 \pm 14.1)\,\mathrm{MeV}/c^2$, and $Y_{\Lambda d} = (4.4 \pm 1.4) \times 10^{-3}/K^-_{stop}$, where the reported width is only the intrinsic one, since the bin width and the spectrometer resolution have been subtracted.

Figure 3 depicts the $\cos\Theta_{\Lambda d}$ distribution for the bump events; *i.e.*, for events in the mass interval $3220 \leq m_{\Lambda d} \leq 3280\,\mathrm{MeV}/c^2$. The distribution is peaked at $\cos\Theta_{\Lambda d} = -1$.

For the same events, the inset of fig. 3 shows the Λ momentum *versus* the d momentum, both of which are centered around $600\,\mathrm{MeV}/c$. Both angular and momentum correlations suggest a back-to-back topology of a slowly moving cluster decaying into a Λd pair. This is also confirmed by the momentum distribution of the Λd pairs, which spans an interval from 50 to $350\,\mathrm{MeV}/c$ (spectrum not shown).

3 The phase space and background reactions

The number of baryons involved in the absorption process suggests that the negative kaon interacts with a ^{3}He-like substructure of ^{6}Li's, thus leaving an undetected $3N$ system in the reaction final state. As shown in fig. 4, if the $3N$ system fully breaks, the $^6\mathrm{Li}(K^-_{stop}, \Lambda d)nnp$ and the $^6\mathrm{Li}(K^-_{stop}, \Lambda d)nd$ phase spaces constrain the $m_{\Lambda d}$ distribution below 3200 and $3240\,\mathrm{MeV}/c^2$, respectively; therefore, these channels can hardly contribute to form the $3251\,\mathrm{MeV}/c^2$ bump.

If the undetected system remains bound, the constraint to belong to the bump requires the kinetic energy of slowly moving tritons to form a peak at $\sim 10\,\mathrm{MeV}$, as shown by the dot-dashed distribution in the fig. 5. Such a peak does not appear in the missing kinetic energy spectrum (solid distribution of fig. 5), which denotes that only a limited strength is available to the $^6\mathrm{Li}(K^-_{stop}, \Lambda d)t$ channel.

A previous work [4] showed that in the capture of K^- by ^{6}Li the nucleus behaves like an $\alpha + d$ system. In this hypothesis, K^- can only be absorbed by the α substructure, therefore, a fast neutron and a spectator deuteron belong to the reaction final state. Based on this assumption, the missing energy of the $^6\mathrm{Li}(K^-_{stop}, \Lambda d)nd$ reaction is the kinetic energy of the nd pairs. The distribution of the energy of the undetected nd pairs (T_{nd}) is reported in fig. 5, and it is depicted up to 90 MeV since above that,

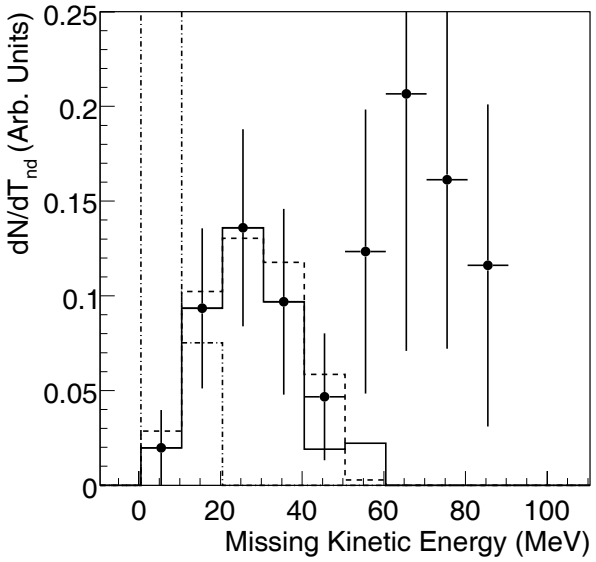

Fig. 5. Measured missing kinetic energy distribution of the ^{6}Li$(K^-_{stop}, \Lambda d)nd$ reaction (experimental points). Solid histogram: missing kinetic energy distribution of the undetected nd events correlated to the mass interval of the bump in fig. 2, namely, $3220 \leq m_{\Lambda d} \leq 3280\,\mathrm{MeV}/c^2$. Dashed histogram: simulated kinetic energy distribution of the undetected nd pairs with the energy of the (spectator) deuteron $T_d < 3\,\mathrm{MeV}$ and the constraint to belong to the bump, namely $3220 \leq m_{\Lambda d} \leq 3280\,\mathrm{MeV}/c^2$, $p_{d,\Lambda} = 600 \pm 200\,\mathrm{MeV}/c$ and $\cos\Theta_{\Lambda d} \leq -0.9$. Dot-dashed histogram: simulated kinetic energy distribution of the undetected t for the ^{6}Li$(K^-_{stop}, \Lambda d)t$ reaction with the same constraints.

$\mathrm{d}N/\mathrm{d}T_{nd}$ is affected by large uncertainties. The distribution presents a bump around 25 MeV. This is found to be strongly correlated to the $3251\,\mathrm{MeV}/c^2$ bump of fig. 2; in fact, a $3220 \leq m_{\Lambda d} \leq 3280\,\mathrm{MeV}/c^2$ cut produces the solid histogram of fig. 5. This occurrence requires a careful kinematic analysis of the undetected nd pairs. To this purpose, the neutron energy distribution is simulated following the ^{6}Li$(K^-_{stop}, \Lambda d)nd$ phase space with the deuteron constrained to be a spectator. Furthermore, the simulated distributions of Λd events are constrained to fit the measured distributions in the ranges $p_{d,\Lambda} = 600 \pm 200\,\mathrm{MeV}/c$, $3220 \leq m_{\Lambda d} \leq 3280\,\mathrm{MeV}/c^2$ and $\cos\Theta_{\Lambda d} \leq -0.9$. The result of the simulations is the dashed distribution in fig. 5, which is normalized to the experimental data. The curve follows closely the behavior of the data, pointing out that most of the kinetic energy is taken away by the undetected neutrons.

4 Conclusions

The present results have been obtained by a comparison among different observables; *i.e.*, Λd invariant mass, momentum, opening angle and nd missing energy. They indicate that in the case of ^{6}Li, the K^-'s are absorbed at rest by α-like substructures, $K^-_{stop}\alpha \to [K^- ppn] + n$, while the remaining deuterons participate to the process as spectators. Final-state neutrons remove the excess energy. The $[K^- ppn]$ clusters finally decay via the $[K^- ppn] \to \Lambda d$ channel.

When $[K^- NNN]$ clusters are discussed in the framework of $\overline{K}$ bound nuclear states, the nuclear ground state of $(K^- \otimes {}^3\mathrm{He} + \overline{K}^0 \otimes {}^3\mathrm{H})$ is predicted to be 108 MeV deep and 20 MeV wide [5]. In this framework, the $[K^- ppn]$ binding energy turns out to be $B_{K^- ppn} = (m_{K^-} + m_p + m_p + m_n) - m_{\Lambda d} = 58 \pm 6\,\mathrm{MeV}$ and $\Gamma_{\Lambda d} = 36.6 \pm 14.1\,\mathrm{MeV}/c^2$, where m is the rest mass of a generic particle. Although the theoretical predictions agree with the experimental findings about the possibility of forming kaonic nuclear states, the quality of the agreement is poor. Further developments both on the theoretical and experimental side are needed.

The present statistics (25 events in the bump) does not permit us to reconstruct data in the low-acceptance region ($m_{\Lambda d} \leq 3160\,\mathrm{MeV}/c^2$). This region is crucial for both understanding the nature of the background and searching for possible deeper bound states. As shown in fig. 4, none of the main background reactions on ^{6}Li leading to final Λd pairs explains the $3251\,\mathrm{MeV}/c^2$ bump, but they are used to fit the lower part of the spectrum. The global fitting results give also the measure of the background contamination, which consists of 6 ± 2 events. In order to take into account the uncertainty in the background estimate, the Uniform Most Power Test [6] was used to calculate the signal significance, which turns out to be 3.9 σ.

With the next data taking, FINUDA will improve the statistical significance of the $3251\,\mathrm{MeV}/c^2$ bump to more than 7σ. Moreover, FINUDA will collect data in the lower-acceptance region, thus allowing a significant study of the background and will even be able to reconstruct a neutron spectrum in coincidence with the Λd particles (about 30 events expected).

References

1. FINUDA Collaboration (M. Agnello *et al.*), Phys. Rev. Lett. **94**, 212303 (2005).
2. FINUDA Collaboration (M. Agnello *et al.*), *FINUDA, a detector for Nuclear Physics at DAΦNE*, LNF Internal Report, LNF-93/021(IR), 1993; FINUDA Collaboration (M. Agnello *et al.*), *FINUDA, Technical Report*, LNF Internal Report, LNF-95/024(IR), 1995.
3. N. Herrmann, *Proceedings of the EXA05 Conference, Vienna 2005* (Austrian Academy of Sciences Press, 2005) ISBN 3-7001-3616-1, p. 73.
4. FINUDA Collaboration (M. Agnello *et al.*), Nucl. Phys. A **775**, 35 (2006).
5. Y. Akaishi, T. Yamazaki, Phys. Rev. C **65**, 044005 (2002).
6. Lehman, *Testing Statistical Hypotheses*, 2nd edition (Wiley, 1986); J.T. Linnemann, arXiv:physics/0312059v2, Dec. 2003.